Accepted for publication in International Journal of Food Microbiology on 9th Jan 2022

A method for non-destructive determination of cocoa bean fermentation levels based on Terahertz hyperspectral imaging

Dinh T. NGUYEN[1,4], Audrey PISSARD[2], Juan Antonio FERNANDEZ PIERNA[2], Hervé ROGEZ[3], Jesus SOUZA[3], Fabian DORTU[1], Saurav Goel[4,5,6], Yves HERNANDEZ[1] and Vincent BAETEN[2]*

[1]*Applied Photonics Department, Multitel A.S.B.L, Rue Pierre et Marie Curie 2, Mons 7000, Belgium*

[2] *Quality and authentication Unit, Knowledge and valorization of agricultural products Department, Walloon Agicultural Research Centre, 24 chaussée de Namur, 5030 Gembloux, Belgium*

[3] *CVACBA (Center for Valorization of Amazonian Bioactive Compounds), UFPA (Federal University of Pará), Avenida Perimetral, 01, 66075-150, Guamá, Belém, Pará, Brazil*

[4] *School of Engineering, London South Bank University, London, SE10AA, United Kingdom*

[5] *Indian Institute of Technology Guwahati, Guwahati, 781039, India*

[6] *University of Petroleum and Energy Studies, Dehradun, 248007, India*

* Corresponding author: nguyed13@lsbu.ac.uk

ABSTRACT

Fermentation of cocoa is a key process to obtain aromatic chocolate products from raw cocoa beans. Hitherto, the levels of fermentation in cocoa are determined using destructive techniques, for example by a cut-test to manually observe the colour inside the beans, or by quantifying ammonia nitrogen (NH_3) in the cocoa powder. In this paper, we present the use of Terahertz hyperspectral imaging as a new way to non-destructively analyse and detect fermented cocoa beans. The study analysed two sets of twenty-two cocoa bean samples with different levels of fermentation from two producers in Brazil. A correlation between fermentation conditions and the outcome results of their THz measurements was observed.

Keywords: *Quality control of cocoa beans, THz imaging, Principal component analysis.*

1. Introduction

Chocolate flavour has been used in the food sector since the discovery of fermentation of cocoa beans. An increase by over 3% demand of cocoa use across the world since 2008 and the production increase from 2.85 million ton in 2000-2001 to 4.84 million tons speaks for the rising demand in this food sector (Beg et al., 2017).

Choosing a premier quality cocoa is an important attribute in the chocolate production. The characteristic of final chocolate products is linked to the fermentation process of cocoa beans. The fermentation quality is dependent on fermentation time (days), temperature or drying method and geographical origin, which governs and influence the quality and taste of the chocolate. Hitherto, it has continued to remain a challenge for the chocolate manufacturers to identify and rapidly screen good quality cocoa.

Nowadays, evaluating commercial grade cocoa beans requires to perform a destructive cutting test of the cocoa beans to count the proportion of purple and brown beans on representative dried samples (Beans, 2015; Santos et al., 2019). However, the cut test is not engineering accurate method and labour oriented as it needs manual counting. For example, (Ilangantileke et al., 1991) presented results of the cut-test score and sensory evaluation methods and it highlighted the variability in results and inadequacies in assessment of the cocoa bean quality.

Another popular method that is commonly used for enhanced quality control of cocoa beans is by quantification of ammonia nitrogen (NH_3) content in the cocoa powder generated during the fermentation due to the degradation of proteins. It is generally quantified by the traditional Conway method (Conway and Flood, 1936). The Conway method measures the absorption of NH_3 volatile matter (VoC) in the air by some reagents (e.g., an acid) which leads to change in the pH value. An alternative to the Conway method is by determining different NH_3 levels in the cocoa powder by using reflectance NIR spectroscopy (Hue et al., 2014). All these methods are destructive and time consuming and can take even upto 48h.

NIR and Fourier Transform NIR (FT-NIR) techniques are quite popular even to estimate the quality of cocoa for example, variety, composition and fraud detection (Barbin et al., 2018; Quelal-Vásconez et al., 2019; Quelal-Vásconez et al., 2018; Sunoj et al., 2016; Teye et al., 2015). However, these methods cannot be considered as ideal as they require the process of powdering the beans, i.e., destroying the cocoa beans before performing the measurements. More recent alternatives include the use of NIR Hyperspectral Imaging that combines NIR spectroscopy and spatial information of the samples. NIR hyperspectral imaging can be directly applied on single cocoa bean for non-destructive prediction of fermentation index, polyphenol content and antioxidant activity (Caporaso et al., 2018) or for the authentication of cocoa bean hybrids (Cruz-Tirado et al., 2020), among others.

Imaging can be also combined with other spectroscopic techniques such as Terahertz (THz). Both THz spectroscopy and imaging are well known non-destructive testing and analysis techniques used in biological (Assefzadeh et al., 2016) and agro-food products, such as the detection of cocoa butter in chocolate (Weiller et al., 2018) and food spoilage evaluation (Hindle et al., 2018). The advantage of THz radiation is that it can reach deeper into the subsurface of non-polar and opaque materials compared to near and mid infrared (IR) ranges. In THz time-domain spectroscopy (THz-TDS) measurements, the electric field amplitude is sampled as a function of time, providing both magnitude and phase spectra. By scanning the sample under the beam, 2D images can be recorded. Valuable information such as refractive index, extinction coefficient, etc. can be extracted from a single THz-TDS measurement in a rapid timeframe. Moreover, recent studies show that NH_3 has fingerprint absorption characteristics in THz range (Assefzadeh et al., 2016) , which opens up an opportunity in this work for quantifying fermentation of cocoa beans using THz technology.

In this paper, we present an approach for using THz time-domain spectroscopy as a novel way for non-destructive evaluation of cocoa bean fermentation levels. For this study, two sets of twenty-two cocoa beans/each processed through different fermentation times from two producers in Brazil were used. The first set of twenty-two beans were used to perform a preliminary study using the THz technology and the second set was used for validation to certify the reproducibility of the results obtained during the first sets of study. For this, THz hyperspectral images of different sets of samples were recorded and analysed using simple statistical models as well as the multivariate analysis e.g., Principal Component Analysis (PCA) method. A correlation between fermentation conditions and the outcome results of their THz measurements was observed which is presented in the results section.

2. Materials and method

2.1. Instrumental setup

This study made use of a THz-TDS system to record hyperspectral images of the samples in transmission mode. The experimental setup is schematically presented in ***Fig. 1(a).*** A mode-locked femtosecond laser (with 100 fs pulse duration, 50 Hz repetition rate, 1550 nm wavelength, and 100 mW average power) was used to pump the photoconductive antenna emitter (*E*) and gate the detector antenna (*R*). A delay line changes the optical path difference between THz and the probe beams, combining coherently at the detector to sample the impulse response signal.

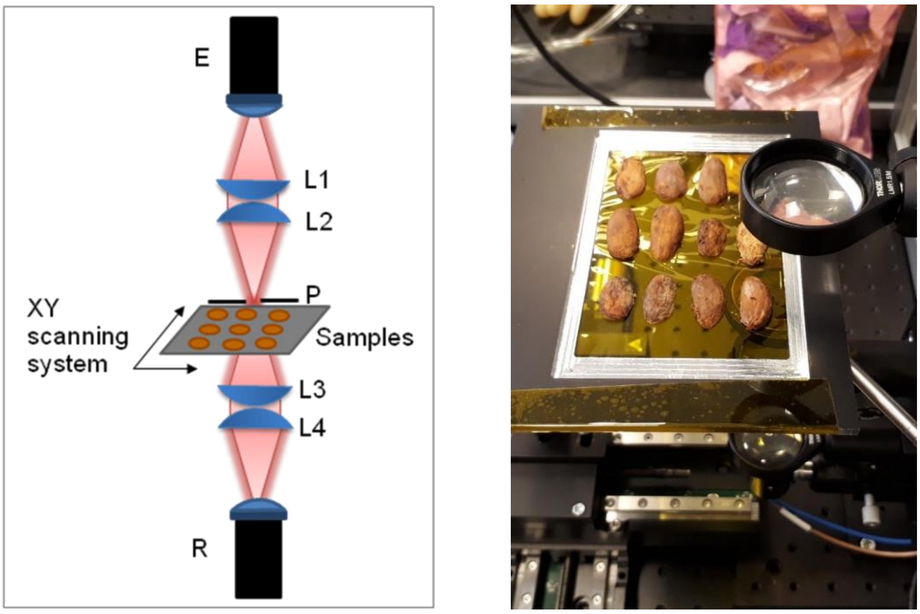

(a) (b)

Figure 1. *(a) Schematic diagram of the TDS system used for cocoa bean measurements in the transmission mode. E and R are THz photoconductive antennas for emitter and receiver respectively. L1, L2, L3, L4 are identical plano-convex lenses. P is a pinhole. (b) Photograph of the cocoa semi-bean samples mounted on the measurement platform.*

Each measurement was performed at room conditions and in the transmission mode, through a 4-f optical setup using four plano-convex lenses (L1-L4) of the same focal length and made of Polymethylpentene material (TPX). Hyperspectral imaging data was obtained by scanning the samples point-by-point. Further details of this instrument setup can be assessed from an alternative source (Nguyen et al., 2018).

A possible mechanism influencing the THz spectroscopic results can be levels of humidity present in the room as THz waves are extremely sensitive to the presence of water. To avoid the effect of humidity on the THz peak-to-peak intensity, a short optical pathlength was deliberately used by choosing appropriate optics which may not be a highly optimal configuration.

2.2. Sample collection

The study used two sets of twenty-two cocoa beans per set processed through different fermentation times (0, 2 and 4 or 7 days). The first set (SET1) of samples was measured in December 2019 and the second set (SET2 or validation set) of samples was measured in June 2020. SET1 was used to perform a preliminary study of THz technology for this kind of data, and SET2 was used as validation to certify the reproducibility of the results obtained with SET1.

The cocoa bean samples were previously cut in half leading to two 'semi-beans'. This step was carried out so that we have one half to perform THz measurements, whilst the other half was kept for further analysis, but the technique also has the potential for its use in a non-destructive manner, e.g., one can always measure the full samples non-destructively by THz measurements. As an exploratory study, the sample details used in this study as SET1 and SET2 are listed in Table 1 and 2 respectively. For each type of sample used, two semi-beans from same fermentation conditions were available for the THz measurements. For every pair of samples, information about fermentation time, height of the fermented layer, as well as the method of drying (mode and time) are shown. Therefore, the THz measurements were realized on 'semi-bean' samples, which were placed on the transparent thin plastic film for 2D scanning, as shown in Figure 1 (b).

Table 1. *Sample list of SET1.*

Sample No.	Fermentation time (days)	Height of fermented layer (cm)	Drying (mode)	Time of drying (days)
1-2	4	20	Not Dried	0
3-4	4	50	Not Dried	0
5-6	7	60	Not Dried	0
7-8	7	60	Shadow	4
9-10	7	60	Sun	3
11-12	7	60	Not Dried	0
13-14	7	60	Sun	3

15-16	0	0	Shadow	3
17-18	0	0	Sun	3
19-20	0	60	Not Dried	0
21-22	0	60	Not Dried	0

Table 2. *Sample list of SET2*

Sample No.	Fermentation time (days)	Height of fermented layer (cm)	Drying (mode)	Time of drying (days)
1-2	0	0	Shadow	4
3-4	0	0	Sun	1
5-6	0	NaN	Not Dried	0
7-8	4	40	Not Dried	0
9-10	4	30	Not Dried	0
11-12	7	60	Shadow	4
13-14	7	60	Not Dried	0
15-16	7	60	Not Dried	0
17-18	2	40	Not Dried	0
19-20	2	30	Not Dried	0
21-22	2	60	Not Dried	0

With the current THz-TDS setup using mechanical delay line, the samples were scanned with a spatial scanning step of 0.4 mm, and it took approximately 6 minutes to finish one seed measurement for the first set and the measurement time was successfully reduced to 4 minutes/sample for the validation set by optimisation of the scanning zone. Scanning time could further be reduced by fully optimising the scanning step. However, the interest of this study is not to optimise the agility of measurement but to obtain the accuracy of measurements and its applicability by performing the feasibility tests.

2.3. Data analysis method

Figure 2 (a) depicts a recorded THz-TDS pulse signal at a single pixel point, from which one can extract the peak-to-peak (*ptp*) magnitude information as follow:

$$\mathbf{ptp} = \mathbf{max}(\,\mathbf{E_{THz}}) - \mathbf{min}(\,\mathbf{E_{THz}}) \tag{1}$$

where E_{THz} is the recorded THz electromagnetic field obtained from the THz-TDS system. Full peak-to-peak image was then mapped in 2D showing substantial contrast depending on the sample properties, as shown in Figure 2(b). Another information that was extracted from the measured THz-TDS pulse signal is the delay time difference between a measured pixel point and that of a reference (the transparent thin plastic film without bean sample). The time-delay difference represents a group refractive index, and can be estimated as:

$$\Delta t = t_{maxSample} - t_{maxRef} \tag{2}$$

where $t_{maxSample}$ is the time-delay (picoseconds) of the maximum measured E-field of the sample whereas t_{maxRef} is that of the reference, and Δt is the difference between these two parameters. Figure 2(c) illustrates how this delay-time difference was calculated.

Figure 2(d) shows a map of the signal amplitude as a function of *y* position along a line through the cocoa bean and the time delay.

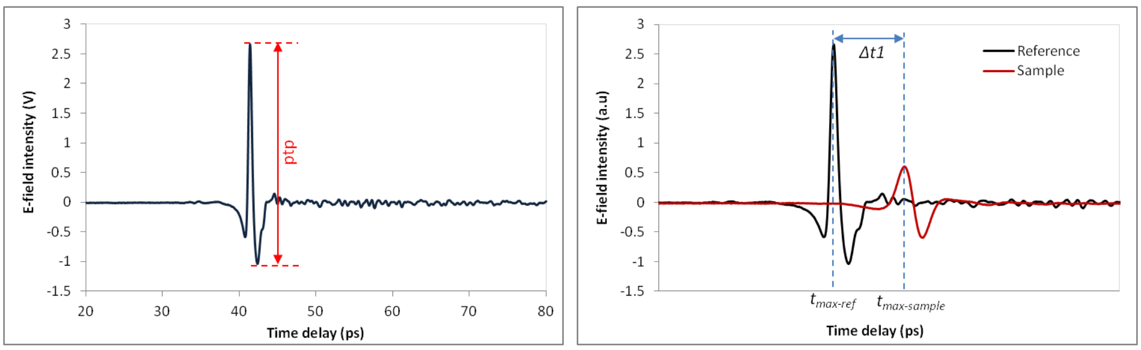

(a) (b)

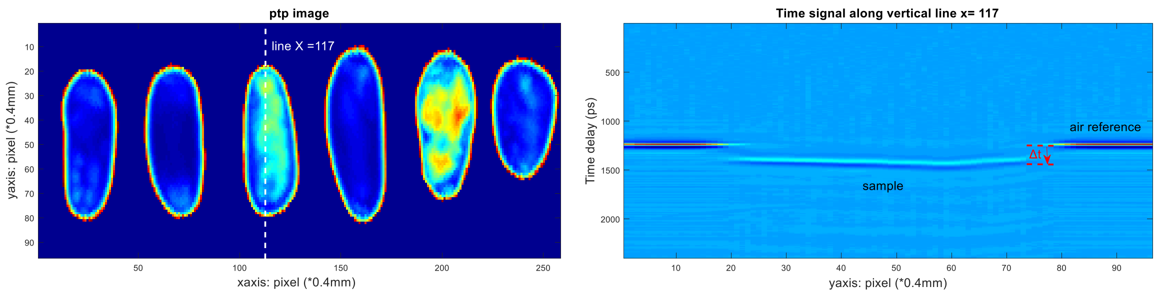

(c) (d)

Figure 2. *(a, b) illustrations of the definitions of the peak-to-peak amplitude and peak-to-peak image of 6 samples; (c,d) illustrations of definition of time-delay difference between sample and reference and time-delay along the marked vertical line in (b). The colour variation in 2(c) indicates the signal intensity received at the detector.*

The shape of a cocoa bean is outlined by putting a threshold to the peak-to-peak information. In this case, we used a threshold of 1.8 V peak-to-peak, meaning any pixel point with peak-to-peak higher than 1.8 V is considered as the plastic film reference, while the remaining pixel points are the cocoa bean points. This threshold was chosen by using the ptp intensity when the signal is transmitted throw plastic film reference itself.

We further calculated the mean and standard deviation of the images for both peak-to-peak and time delay as specific quantitative classification parameters. The mean, μ, was calculated by averaging pixels' values of all the beans as:

$$\boldsymbol{\mu}_{\mathbf{time}} = \frac{\sum \Delta \mathbf{t_i}}{\mathbf{N}} \qquad (3)$$

$$\boldsymbol{\mu}_{\mathbf{magnitude}} = \frac{\sum \mathbf{ptp_i}}{\mathbf{N}} \qquad (4)$$

where Δt_i and ptp_i are the time-delay difference (in picoseconds) and peak-to-peak value (V) respectively of pixel i and N is the number of pixels. Similarly, the standard deviation (σ) of a sample was calculated as follow:

$$\boldsymbol{\sigma}_{\mathbf{time}} = \sqrt{\frac{(\Delta \mathbf{t_i} - \boldsymbol{\mu}_{\mathbf{time}})^2}{\mathbf{N}}} \tag{5}$$

$$\boldsymbol{\sigma}_{\mathbf{magnitude}} = \sqrt{\frac{(\mathbf{ptp_i} - \boldsymbol{\mu}_{\mathbf{magnitude}})^2}{\mathbf{N}}} \tag{6}$$

where μ is mean of the N sample population.

To compare the tolerance of the standard deviation to the mean of each sample, T parameter can be calculated for both time delay and peak-to-peak as:

$$T_{time} = \sigma_{time} / \mu_{time} \times 100\ \% \tag{7}$$

$$T_{magnitude} = \sigma_{magnitude} / \mu_{magnitude} \times 100\ \% \tag{8}$$

The tolerance T is dependent on both σ and μ, therefore we can representatively use σ and T in data analysis for qualification of the samples.

3. Results and discussions

3.1. Analysis of Samples in SET1

The available twenty-two cocoa bean samples of SET1 were first measured and analysed for the time-delay difference and peak-to-peak magnitude at each pixel. Pixels with peak-to-peak value higher than the pre-determined threshold for our measuring system (1.8V) were from the plastic film reference and are, then, referenced to zero. Figure 3 shows the images of the peak-to-peak amplitude of the 22 cocoa beans. The 22 samples are placed from top to bottom in the same order as in Table 1 (i.e., 11 pairs from 1 to 11 containing each 2 semi-beans). A clear qualitative difference was observed between the non-fermented samples (with 0 day of fermentation time) compared to the other samples.

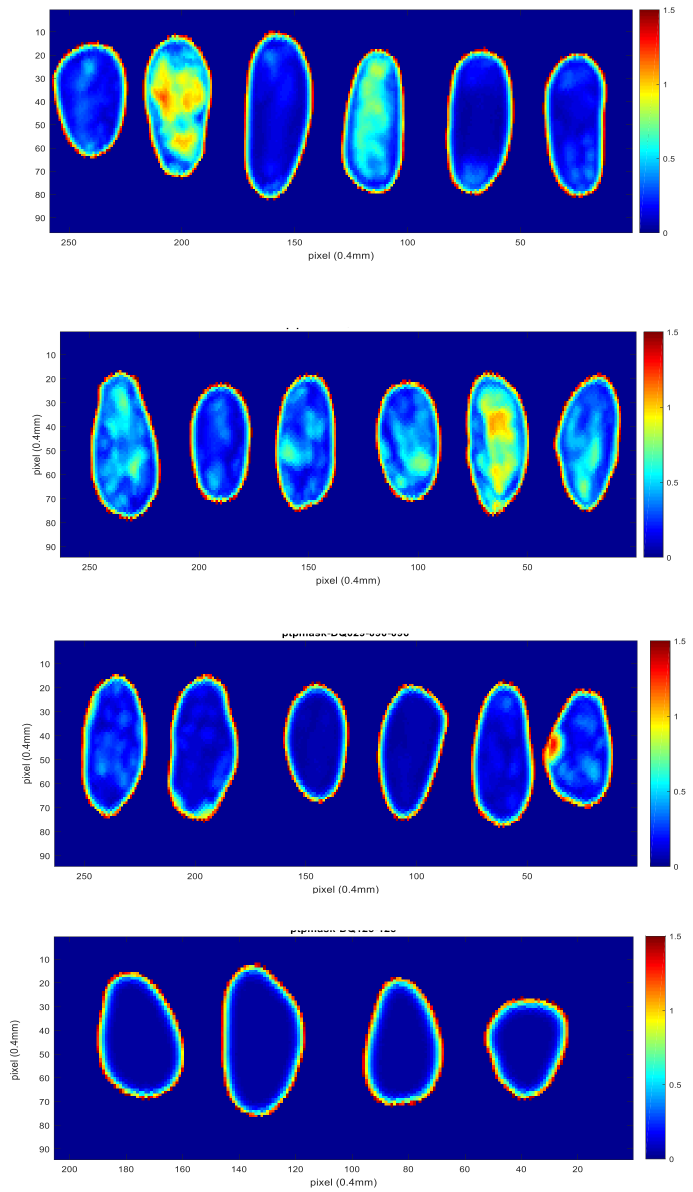

Figure 3. Images of time-delay difference (between the sample and the thin plastic film reference) of the 11 pairs of samples.

The mean μ and standard deviation σ were then calculated for each cocoa bean sample. The results are plotted in Figure 4(a) showing μ_{time} vs. σ_{time} for group of samples collated together according to their fermentation time, fermentation height and drying time and method. A distinct difference was seen between the non-fermented samples (the squared dots) and those with different fermentation levels. The other samples of different fermentation heights (in cm) were not very well separated in this study. In particular, the non-fermented samples were divided in two groups apparently according to the drying process, i.e., not dried versus dried samples (with sun or shadow).

It may be noted that the non-fermented and non-dried samples were clearly distinct from the remaining samples. On the other hand, the fermented samples (4 or 7 days) were clustered together without any differentiation. As time is reciprocal of frequency, the time parameters such as μ_{time} and σ_{time} are related to physical and chemical characteristics in THz frequency range of the samples. Therefore, this result may be linked to the strong absorption peak of NH_3 in the THz range. However, for further research and development, both experiment and data analysis will need to be done for better understanding the mechanisms influencing the THz results, especially if it is related to the fermentation heights of the samples.

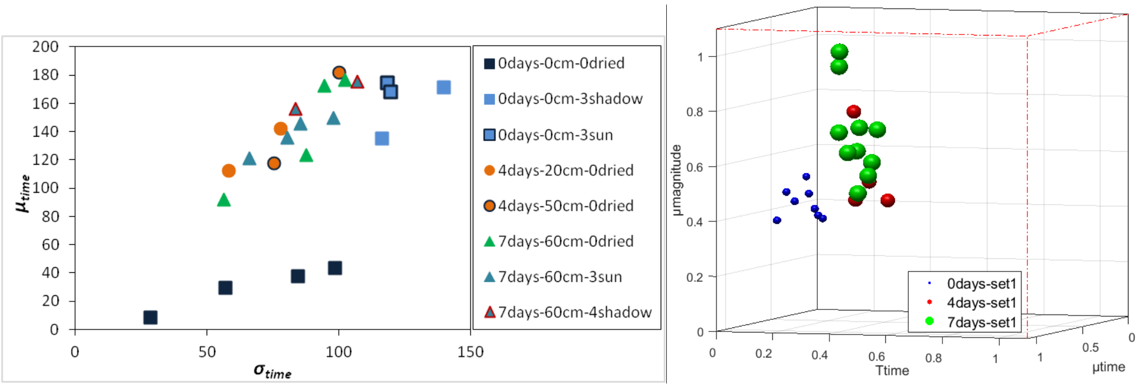

Figure 4. *SET1: (a) Calculated μ_{time} vs. σ_{time} of the samples for different fermentation conditions (time in days, height in cm, and dried day and method); (b) 3D plot of normalised μ_{time} vs. T_{time} vs. $\mu_{magnitude}$.*

For this study, we focus on qualifying the most important fermentation condition which is the fermentation time. Figure 4(b) plot shows a 3D view of the indices μ_{time} vs. T_{time} and vs. $\mu_{magnitude}$ of Set1 samples in which the samples were grouped based on their fermentation time (in days). To demonstrate fairly the influence of fermentation time to the measured THz indexes, the parameters were normalized before plotting. It showed a distinct separation in the second dimension (T_{time}) of non-fermented (0 day) vs. the fermented samples (4 or 7 days). In the following analysis, the samples were grouped based on the fermentation time only.

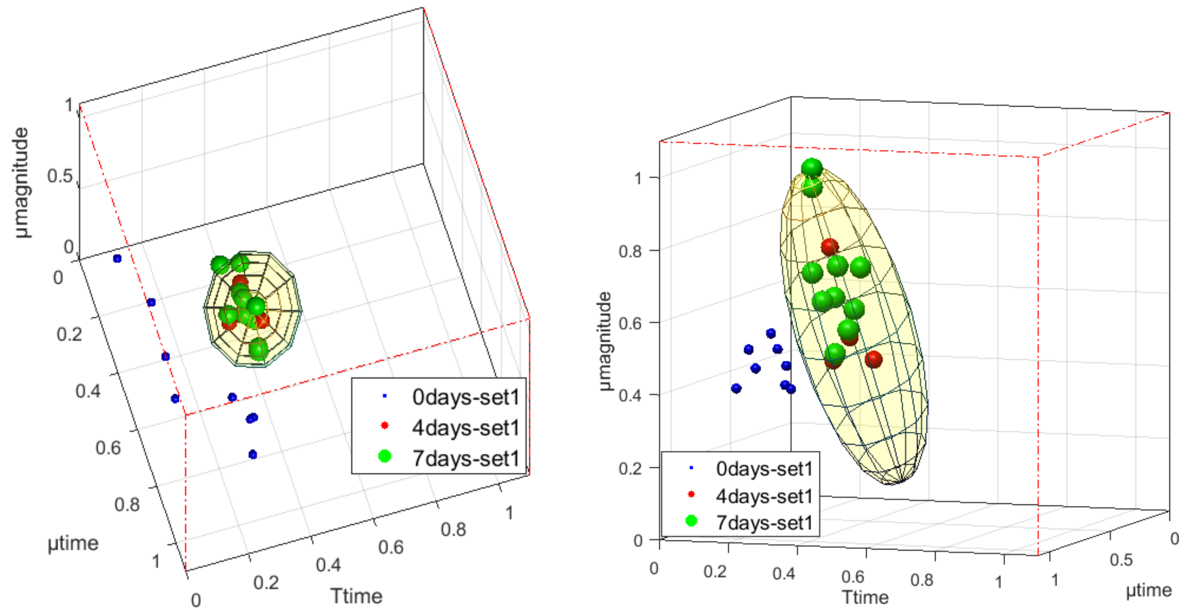

Figure 5. *Comparison of samples obtained from SET1 using normalised parameters* **(**μ_{time} *vs.* T_{time} *vs.* $\mu_{magnitude}$*) and a fitting ellipsoid covering the fermented samples.0*

In Figure 5, an ellipsoid fitting was calculated to cover all the fermented samples. If we use this ellipsoid as a determined threshold to separate fermented and non-fermented samples, the prediction was 100% matching to all the samples used in SET1.

3.2. Analysis of second sets of samples (SET2) used for validation

To further validate the results obtained from SET1 samples and to understand the relation between different THz indexes and fermentation time, a second set (validation set) was measured and analysed. This validation set (SET2) consists of 22 different cocoa semi-bean samples as per Table 2.

Figure 6 compares SET1 and SET2 results. The same ellipsoid threshold calculated with SET1 was used to qualify the samples in SET2 for validation. Using the predefined standard, two mismatching cases were detected which are circled in red (one 2 days fermented sample is in non-fermented zone and one non-fermented sample is in the fermented zone).

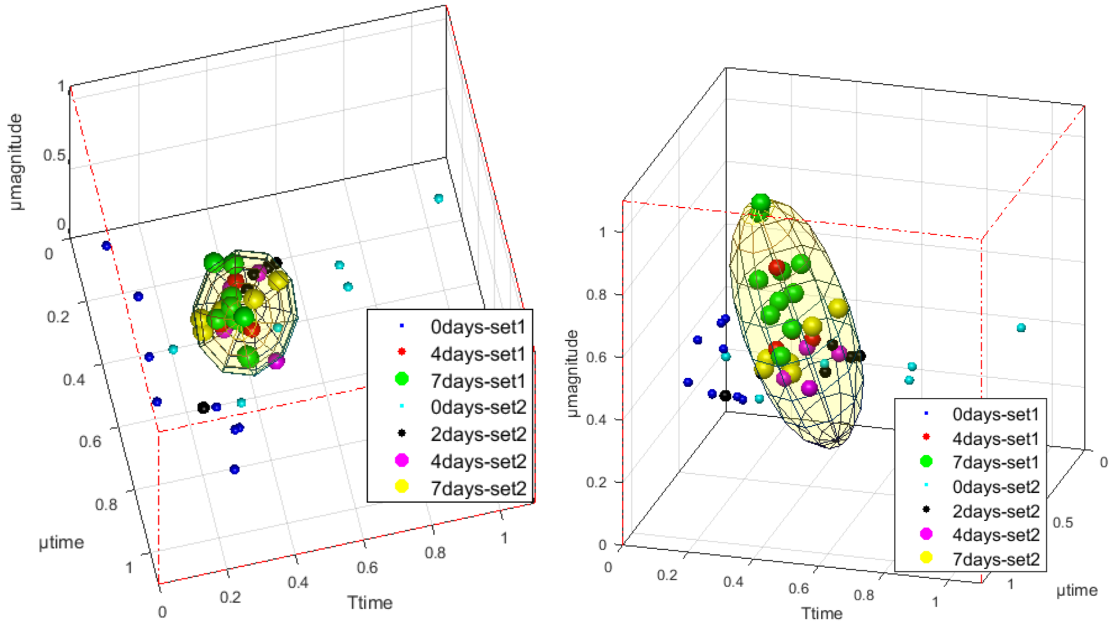

Figure 6. *Comparison of SET1 vs. SET2: 3D plot of normalised μ_{time} vs. T_{time} vs. $\mu_{magnitude}$ and fitting ellipsoid threshold of fermented samples in SET1.*

To further investigate the data in 4 dimensions (μ_{time}, T_{time}, $\mu_{magnitude}$ and $T_{magnitude}$) principal components analysis (PCA) was deployed. The PCA was applied to all four parameters by normalising the parameters prior to applying the PCA. Figure 7 shows 3D plot revealing the scores of the first three principal components and a fitting ellipsoid for fermented samples. The first three components scored 96.3% which could be highly representing the data. From Figure 7 one can see that the fermented samples tend to be centred inside the ellipsoid whereas the non-fermented samples remain isolated and farther from the central region. There are two mismatching cases circled in red. The PCA calculation shows the same results as the study with three parameters (μ_{time} vs. T_{time} vs. $\mu_{magnitude}$).

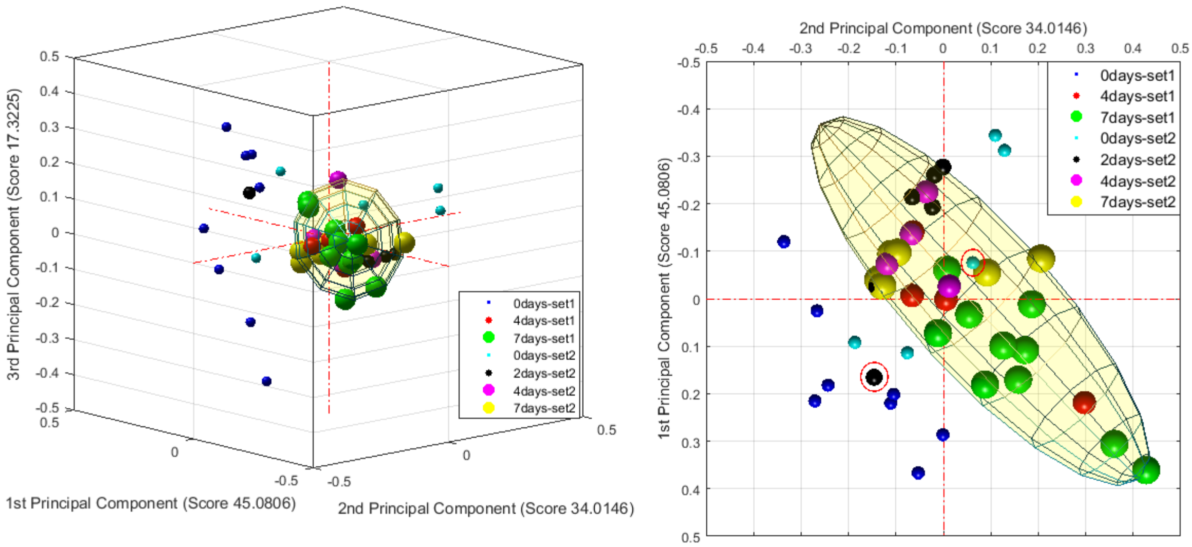

Figure 7. *Principal components analysis applied to Set1 and Set2: 3D plots of the first 3 principal components for analysis applied on 4 parameters: μ_{time}, T_{time}, $\mu_{magnitude}$ and $T_{magnitude}$ and a fitting ellipsoid covering the fermented samples. The two samples marked in red circles are mismatching cases.*

From Figure 7 one can see that samples of the same fermentation time grouped together (0, 2, 4 and 7 days) represented a unique cluster. In both measurements, non-fermented samples remained identifiable distinctly compared to the fermented samples. Samples with a high fermentation level occupied more centred distribution whereas non-fermented beans showed a large, scattered divergence away from the centre.

Finally, using the same ellipsoid threshold, we can correctly predict 20 out of 22 samples for SET2, giving 90.9% matching cases (the 2 samples in marked red circles are mismatching cases). It is obvious that higher the population (number of samples), the better thresholds can be calculated and the nearer we can reach to the true percentage of matching cases. For example, if we count both SET1 and SET2 for the calculation, we correctly predicted 42 out of 44 samples, making it 95.45% matching cases. As first feasibility study, it was successfully demonstrated in this work that the use of THz technology for quality control of cocoa beans can become a robust game changing technology offering better agility.

Improvement in confidence level is possible by further optimisation of the technique which will be pursued in the follow-on work. This would particularly be beneficial and crucial to apply to the emerging nanomanufacturing problems (Fan et al., 2021; Khatri et al., 2020; Kumar Mishra et al., 2021)

4. Conclusions

A new measurement system was developed to characterise the fermentation levels in the cocoa beans with an improved agility than the currently used methods used in this sector. Our novel method involving the use of THz hyperspectral imaging showed new prospects for deploying this technique as an industrial practice as a key non-destructive technique for improved quality assurance for the chocolate business. Measurements involving two different datasets obtained at different time periods helped to gain the confidence in the data which proved to be a strong validation of the key results obtained and reported here. In this study, it took about 4 minutes per sample of cocoa bean for its characterisation, but this time window can further be squeezed by optimisation of the technique. The results show a distinct difference between fermented and non-fermented samples, with prediction accuracy of 95% while testing 44 samples.

The work has opened new possibilities in the arena of non-destructive and agile measurement techniques to reliably characterise industrial crops, cereals and many other products used commonly in the food sector.

Acknowledgement

This work was done under Tera4All project. We express great thanks to the Fédération Wallonie Investissent and En Mieux for their support. Additional thanks to BELCOBRA (Brazil-Belgium cooperation CAPES-WBI/2017-2019/361394) for financing the project: ‘Optimization and implementation of analytical methods for the traceability and authenticity of cocoa and chocolate’ from which the samples were prepared. This project is coordinated by CRA-W and UFPA. Authors are grateful to CEPLAC (Medicilandia, PA, Brazil) for the mature fruits, to Teixeira L.E.O. and Freitas A.L. (UFPA) for their technical assistance for fermentation and drying process, and to Quentin Arnould (CRA-W) for laboratory support.

SG greatly acknowledge the financial support provided by the UKRI via Grants No. EP/L016567/1, EP/S013652/1, EP/S036180/1, EP/T001100/1 and EP/T024607/1 and from the TFIN+ Feasibility study award to LSBU (EP/V026402/1), the Royal Academy of Engineering via Grants No. IAPP18-19\295 and TSP1332, EURAMET EMPIR A185 (2018), the EU Cost Action (CA15102, CA18125, CA18224 and CA16235) and the Newton Fellowship award from the Royal Society (NIF\R1\191571).

References

Assefzadeh, M.M., Jamali, B., Gluszek, A.K., Hudzikowski, A.J., Wojtas, J., Tittel, F.K., Babakhani, A., 2016. Terahertz trace gas spectroscopy based on a fully-electronic frequency-comb radiating array in silicon, 2016 Conference on Lasers and Electro-Optics (CLEO). IEEE, pp. 1-2.

Barbin, D.F., Maciel, L.F., Bazoni, C.H.V., da Silva Ribeiro, M., Carvalho, R.D.S., da Silva Bispo, E., Miranda, M.d.P.S., Hirooka, E.Y.J.J.o.f.s., technology, 2018. Classification and compositional characterization of different varieties of cocoa beans by near infrared spectroscopy and multivariate statistical analyses. 55, 2457-2466.

Beans, C., 2015. Cocoa Beans: Chocolate & Cocoa Industry Quality Requirements.

Beg, M.S., Ahmad, S., Jan, K., Bashir, K.J.T.i.f.s., technology, 2017. Status, supply chain and processing of cocoa-A review. 66, 108-116.

Caporaso, N., Whitworth, M.B., Fowler, M.S., Fisk, I.D.J.F.c., 2018. Hyperspectral imaging for non-destructive prediction of fermentation index, polyphenol content and antioxidant activity in single cocoa beans. 258, 343-351.

Conway, E.J., Flood, J.C.J.B.J., 1936. An absorption apparatus for the micro-determination of certain volatile substances: The micro-determination of bromide, with application to blood and urine and observations on the normal human subject. 30, 716-727.

Cruz-Tirado, J., Pierna, J.A.F., Rogez, H., Barbin, D.F., Baeten, V.J.F.C., 2020. Authentication of cocoa (Theobroma cacao) bean hybrids by NIR-hyperspectral imaging and chemometrics. 118, 107445.

Fan, P., Goel, S., Luo, X., Upadhyaya, H.M.J.N., Metrology, 2021. Atomic-Scale Friction Studies on Single-Crystal Gallium Arsenide Using Atomic Force Microscope and Molecular Dynamics Simulation. 1-11.

Hindle, F., Kuuliala, L., Mouelhi, M., Cuisset, A., Bray, C., Vanwolleghem, M., Devlieghere, F., Mouret, G., Bocquet, R.J.A., 2018. Monitoring of food spoilage by high resolution THz analysis. 143, 5536-5544.

Hue, C., Gunata, Z., Bergounhou, A., Assemat, S., Boulanger, R., Sauvage, F.-X., Davrieux, F.J.F.c., 2014. Near infrared spectroscopy as a new tool to determine cocoa fermentation levels through ammonia nitrogen quantification. 148, 240-245.

Ilangantileke, S., WAHYUDI, T., BAILON, M.G.J.J.o.f.q., 1991. Assessment methodology to predict quality of cocoa beans for export. 14, 481-496.

Khatri, N., Barkachary, B., Muneeswaran, B., Al-Sayegh, R., Goel, S., 2020. Surface Defects incorporated Diamond Machining of Silicon. International Journal of Extreme Manufacturing.

Kumar Mishra, R., Goel, S., Yazdani Nezhad, H., 2021. Computational prediction of electrical and thermal properties of graphene and BaTiO3 reinforced epoxy nanocomposites. Biomaterials and Polymers Horizon 1, 1-14.

Nguyen, D., Dortu, F., Dispa, A., Hubert, P., Ziemons, E., Hernandez, Y., 2018. Terahertz hyper-spectral imaging of lab-prepared versus commercial paracetamol tablets and potential applications, Unconventional Optical Imaging. International Society for Optics and Photonics, p. 106773I.
Quelal-Vásconez, M.A., Lerma-García, M.J., Pérez-Esteve, É., Arnau-Bonachera, A., Barat, J.M., Talens, P.J.F.C., 2019. Fast detection of cocoa shell in cocoa powders by near infrared spectroscopy and multivariate analysis. 99, 68-72.
Quelal-Vásconez, M.A., Pérez-Esteve, É., Arnau-Bonachera, A., Barat, J.M., Talens, P.J.F.C., 2018. Rapid fraud detection of cocoa powder with carob flour using near infrared spectroscopy. 92, 183-189.
Santos, F.A., Palmeira, E.S., Jesus, G.J.D.i.b., 2019. An image dataset of cut-test-classified cocoa beans. 24, 103916.
Sunoj, S., Igathinathane, C., Visvanathan, R.J.C., Agriculture, E.i., 2016. Nondestructive determination of cocoa bean quality using FT-NIR spectroscopy. 124, 234-242.
Teye, E., Huang, X., Sam-Amoah, L.K., Takrama, J., Boison, D., Botchway, F., Kumi, F.J.F.c., 2015. Estimating cocoa bean parameters by FT-NIRS and chemometrics analysis. 176, 403-410.
Weiller, S., Tanabe, T., Oyama, Y.J.W.J.o.E., Technology, 2018. Terahertz non-contact monitoring of cocoa butter in chocolate. 6, 268.